The Effect of Redlining on Ethnic Pollution Disparities*

Julian Wichert[1] and Richard Bluhm[2]

[1] *Leibniz University Hannover*
[2] *University of Stuttgart*

August 2022
PRELIMINARY, PLEASE DO NOT CIRCULATE

Abstract

Have discriminatory housing policies contributed to today's ethnic pollution disparities? We examine the impact of "Redlining" during 1930s in the US which assigned risk grades to neighborhoods according to housing characteristics and ethnic composition on spatial patterns of urban air pollution. We apply a methodology that uses propensity scores in a boundary design to hyper-local air quality measurements. The correlative results across urban neighborhoods clearly show that a better neighborhood grade historically is associated with lower air pollution today. Our very preliminary causal boundary results are suggestive of a locking-in of ethnic pollution disparities.

JEL-classification: Q53, R23, J15

Keywords: Air Pollution, Urban Economics, Economics of Minorities

*The authors greatly appreciate helpful comments from participants at: Beyond Basic Question Workshop and UC San Diego's GPS Environment and Policy Group Seminar.

1 Introduction

In many high-income countries, air quality has improved tremendously over the last decades thanks to stringent environmental policies and innovations in transportation, power generation and manufacturing. Yet, considerable levels of air pollution remain which can lead to respiratory illness, cardiovascular disease and adverse health outcomes of newborns. Strikingly, for the United States the burden is still unequally born across ethnic groups (Colmer et al., 2020; Riddell et al., 2022; Liu et al., 2021; Ash and Boyce, 2018; Gillingham and Huang, 2021). Besides residential sorting along existing pollution gradients, it has been suggested that in the US, public policy might have contributed to the ethnic environmental disparity. In particular "redlining", the discriminatory practice by a US federal agency in the 1930s which consisted of labelling neighborhoods according to credit worthiness is conjectured to have amplified pollution disparities. The repercussions might last until today due to the new siting of polluting industries and of transportation pathways. Several recent studies have provided evidence that neighborhoods which received an unfavorable risk grade in the 1930s still have higher levels of air pollution today (Tessum et al., 2019; Nardone, Casey, Morello-Frosch, Mujahid, Balmes and Thakur, 2020; Namin et al., 2020; California EPA, 2021). However, these studies are only correlational, not accounting for pre-existing disparities between neighborhoods prior to the labelling during the 1930s (**?**Fishback et al., 2021). Hence, it is unclear to which degree today's ethnic pollution disparities can be causally attributed to the historical urban policy. We aim to fill this gap in a boundary setting via propensity score methods using hyper-local air quality measurements.

2 Background on Redlining

After the Great Depression, a US federal agency, the Home Owners' Loan Corporation (HOLC), hired real estate contractors to assess the riskiness of lending according to neighborhoods in over 200 cities. Neighborhoods were classified into four groups, based on housing characteristics like housing age, quality, occupancy, prices and non-housing characteristics like race, ethnicity, and immigration status. An example of such an assessment for one neighborhood in Los Angeles is provided in Figure 10 in the Appendix. Each assessment was summarized by a final grade ranging from letter A (reflecting a good risk grade) to D (reflecting high risk). The grades for all neighborhoods were combined to risk maps for each city that was larger than 40,000 inhabitants (see Figure 9 for an example of such a map for Los Angeles). The risk grades were color-coded, from green reflecting good standing, to blue, yellow to red (bad standing).

An beorgeoing field of the literature discusses the implementation of the HOLC maps during the 1930s its lasting repercussions until today. Rothstein (2017) argues that HOLC's redlining maps had a huge impact on mortgage access. Fishback et al.

(2021) assess loan data by the HOLC between 1933–1936 and by the Federal Housing Administration (FHA) between 1935–1940 in three US cities. Overall, they find the same exclusionary pattern in loan-giving before and after the HOLC and FHA programs during the 1930s. **?** exploit random idiosyncrasies in the map boundaries within neighborhoods to provide causal evidence for 149 cities that the redlining-practice had an amplifying effect on within-city segregation and housing outcomes.

The area description files also mention environmental factors that might have counted towards the overall grade assignment. The Underwriting Manual of the FHA in 1936 classified the occupancy of ethnic groups in the same category as pollution hazards. According to the Manual, green-space was considered to contribute to a better grade: "A location close to a public park or area of similar nature is usually well protected from infiltration of business and lower social occupancy coming from that direction." Moreover, "A high-speed traffic artery or a wide street parkway may prevent the expansion of inharmonious uses to a location on the opposite side of the street.". California EPA (2021) notes that the configuration of laws promoted the (re-) location of polluting land uses towards neighborhoods with unfavorable risk grade. Rothstein (2017) argues that zoning laws "attempted to protect white neighborhoods from deterioration by ensuring that few industrial or environmentally unsafe businesses could locate in them. Prohibited in this fashion, polluting industry had no option but to locate near African American residences ."

Hoffman et al. (2020) find that urban heatwaves today hit historically redlined neighborhoods disproportionately stronger than their non-redlined counterparts. On average, they are 2.6°C hotter. (Nardone, Casey, Morello-Frosch, Mujahid, Balmes and Thakur, 2020) examine birth outcomes within three US cities. They show that formerly redlined neighborhoods have elevated levels of low birth weight and preterm birth. Nardone, Casey, Rudolph, Karasek, Mujahid and Morello-Frosch (2020) use emergency department visits between 2011 to 2013 in 8 cities and find higher occurrence of asthma incidences in redlined neighborhoods.

3 Data and Empirical Strategy

3.1 Empirical strategy

One major empirical issue that any empirical analysis about redlining faces is the fact that neighborhoods were already different prior to the drawing of the risk maps. We follow **?**, who apply propensity score methods in a boundary approach to account for that.

The first step to come closer to a causal effect of redlining on pollution disparities is to focus on narrow neighborhood bands around the border between two differently graded neighborhoods. Instead of running regressions across whole neighborhoods, we, thus, focus on areas that have similar access to urban amenities like schools, parks or shopping. This boundary approach is illustrated for Los Angeles in Figure

Figure (1) Boundary approach for B-C boundaries

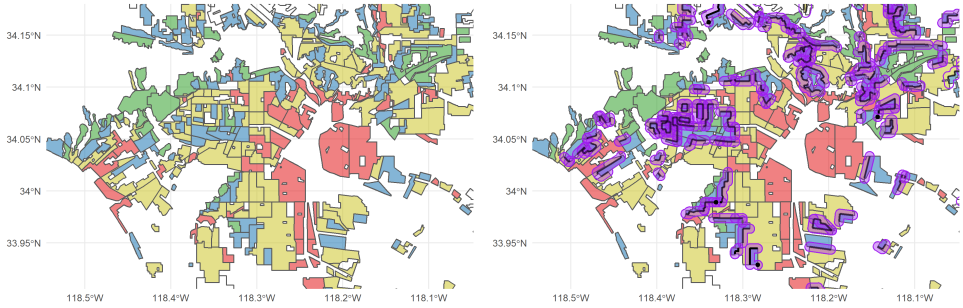

(a) HOLC polygons in LA (b) HOLC B-C boundary segments

1.

In a naive approach, one would compare air quality within these 400m-buffers on either side of a boundary:

$$y_{gbc} = \beta \, \mathbf{lgs_{gb}} + \alpha_b + \epsilon_{gbc}$$

where y_{gbc} is the air quality in a geographic unit g (the 'buffer') on boundary b, in city c, lgs_{gb} is an indicator that the geographic unit g is on the lower-graded side of the HOLC boundary b, α_b are fixed effects for boundary segments.

The strong assumption one would need to impose to derive a causal estimate states: In the absence of the HOLC maps, level and trend differences on the boundaries must be negligible. Guided by the results of **?** one must reject that assumption. For instance, the authors show that, along C-D boundaries between 1910-1930, population composition trended differently on either side of boundary. Moreover, there was a widening gap in housing variables like homeownership, house values, rents before the treatment. This pre-existing difference was similar at B-C boundaries. Regarding pollution sources, it is not fully clear whether there were pre-existing differences across the boundaries but we it is more likely than not. Hence, the naive estimates from the above regression would only reflect correlations, not the causal effect of the HOLC maps.

The study by **?** that we rely on for this analysis resolves this issue in two different ways: In the first approach, we use the actual treatment boundaries but contrast them against a more plausible set of comparison boundaries: We detect potential comparison boundaries that had high treatment likelihood based on a propensity score but were, in fact, not treated. These comparison boundaries are grid lines that lie *within* HOLC polygons, not at actual HOLC boundaries. This is illustrated in Figure **??** in the appendix. Thus, we compare two groups of boundaries that had similar treatment likelihood ex-ante, only one of which was treated in virtue of becoming a HOLC boundary. In the second approach, we exploit "quirks" in the drawing of the HOLC boundaries, that is, de facto boundaries that had an ex-ante low likelihood of being treated based on their propensity scores.

Regarding this first approach, the steps to allocate the comparison boundaries are as follows: We start by drawing a random "grid" across each city. We treat the grid lines as boundaries. Next, we compute propensity scores along all boundaries based on the treatment status (1 for de facto treated boundaries, 0 for the grid lines) and on differences in the 400m-buffers around the boundaries. The propensity scores are derived from the predicted probabilities of treatment in a probit-regression:

$$\mathbf{1}\{Treated\}_{bc} = \alpha_c + \sum_{k=1}^{K} \beta_{pre}^{k} (x_{lgs} - x_{hgs})_{bc}^{k,pre} + \epsilon_{bc}$$

where $(x_{lgs} - x_{hgs})$ reflect differences in characteristic k prior to treatment: population composition, e.g. share of African American, African American population density, white population density, share foreign born and housing variables, e.g. homeownership rate, share homeowner with mortgage, log(house value), log(rent).

Figure (2) Treatment likelihood at B-C boundaries

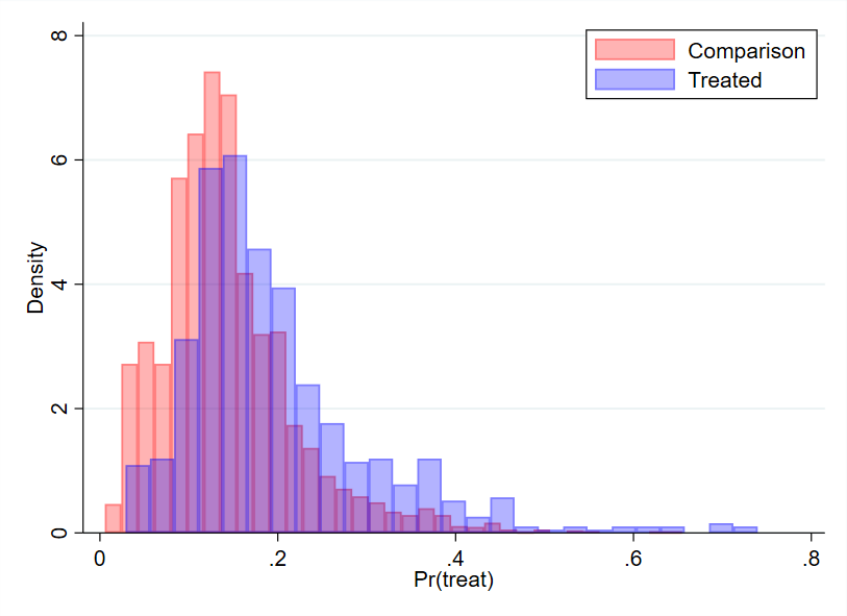

Notes:

Figure 2 shows a density plot of propensity scores, separately for treated (blue) and comparison boundaries (red). There two things to note: First, there is considerable overlap in the treatment propensity between the two sets of boundaries. This is an important requisite for the analysis as it shows that there are many urban boundaries with a similar treatment probability where one group was eventually treated (blue) and another group was not treated (red). The second feature to note is that the lines that were eventually treated had an ex-ante higher treatment likelihood, reflected in the figure by the shift of the distribution to the right. This calls for an adjustment according to the treatment propensity.

The resulting regression approach is this:

$$y_{gbc} = \beta_{lgs \cdot treated} \ \left(\mathbf{lgs}_{gb} \text{ x } \mathbf{Treated}_b\right) + \gamma \ \mathbf{lgs}_{gb} + \alpha_b + \epsilon_{gbc}$$

where y_{gbc} is air pollution in 400m-buffer g on boundary b, in city c, lgs_{gb} is an indicator whether the buffer g is on the lower-graded side of the HOLC boundary b, $Treated_b$ is an indicator whether the boundary b is a HOLC boundary, $\mathbf{lgs}_{gb}$ x $Treated_b$ gives the treatment effect, α_b are fixed effects for boundary b. The treatment probabilities are used as follows: Treatment boundaries receive weight $w = 1$, while the comparison boundaries receive weight $w = \frac{pscore}{1-pscore}$. This up-weights potential boundaries with high ex-ante high treatment likelihood (e.g. high racial cleavages, high occupation disparities).

The second approach, illustrated in Figure 12 in the appendix, is motivated by the observation that some boundaries are "random", only drawn to close a polygon. Those treated boundaries do not reflect systematic differences, and are, thus, much less likely to show pre-trends in outcomes. In terms of identification this means that we exploit variation only from those boundaries which had a low likelihood of being treated based on observables. In this sense, the drawing of a HOLC boundary between those buffers can be seen as a "surprise treatment". We implement this idea by only using those boundaries with propensity scores below the median.

3.2 Data

Pollution. This analysis has specifically high requirements regarding the spatial granularity of the data. Yet, the better the spatial resolution, the lower the overall coverage of the data. We explain the different measures of air quality in order of declining coverage and increasing granularity:

As the first source, the PM2.5 data by Meng et al. (2019) is a yearly grid dataset for the whole US at 0.01°x0.01° (ca. 1km) resolution. Their estimates are based on various ground-station and satellite measurements that are combined using chemical transport models. They even extend the panel backwards to cover the period 1981-2016. Second, we use PM, $Ozone$ measurements from low-cost sensors. Purple Air sensors are privately installed devices, the coverage increased strongly in 2018, with 25,000 monitors currently installed in US, alone 6,000 monitors are in California. These sensors record air pollution measurements every 2min. The Purple Air sensors can be combined with 510 EPA Sensors for PM, AQI. Methodological studies to validate the Purple Air devices include Barkjohn et al. (2019); Feenstra et al. (2020); Tryner et al. (2020). The third source of air quality measurements comes from mobile sensors. A few of Google's Street View vehicles record particle counts for NO_2, PM, Ultra Fine Particles (UFP), $BlackCarbon$ and $Ozone$. With 60 measurements per minute, this yields in 42 million observations and hyper-local granularity. Figure 15 shows the exemplary measurements for one vehicle. These mobile measurements are only available for cities in California's Bay Area, see Figure 17, and several

neighborhoods in Los Angeles, see Figures 16. Technical guidance using the mobile station data is provided in the publication by Apte et al. (2017). The data have been linked to health outcomes in the studies by Alexeeff et al. (2018); Riddell et al. (2022). Mobile sensors have also found application in data-scare development context, for example in Ugandan cities (Bassi et al., 2021).

Figure (3) HOLC Purple Air Sensors

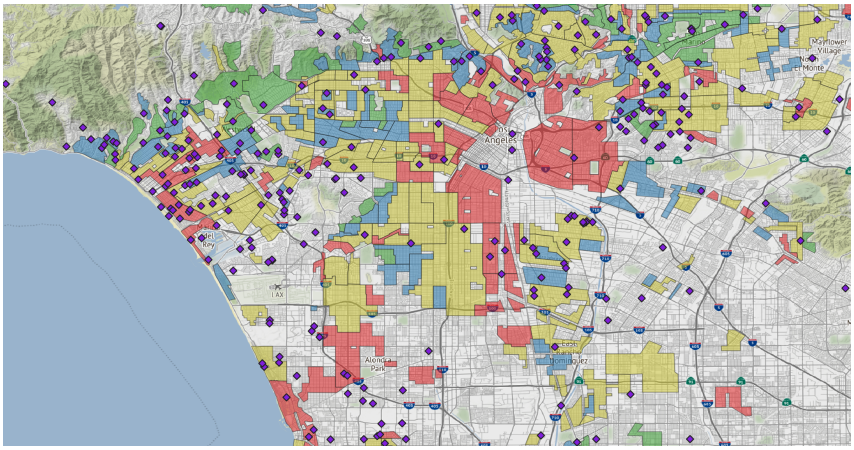

Notes: Purple dots reflect the location of Purple Air Sensors across Los Angeles. The colored polygons indicate the HOLC grades for neighborhoods in Los Angeles.

Redlining. As another main input to the analysis we use the georeferenced HOLC maps for 149 US cities. Moreover, we currently apply for the US 1940 full-count census that is precise to the address level.

Other. Moreover, we plan to use granular data on the freeway expansion, including the opening dates of new segments (Brinkman and Lin, 2020; Baum-Snow, 2020).

4 Results

To start off, we show correlational evidence on the relationship between the air pollution in entire neighborhoods and their and HOLC grades. Figure 4 shows results from an OLS regression of air pollution on HOLC grades[1]:

Figure 4 shows the results for PM2.5-pollution with three different measurements. For the gridded pollution product in Panel (a): While A-graded neighborhoods have the lowest level of PM2.5, B- and C- graded neighborhoods have a higher level of pollution. Panel (b) shows the neighborhoods-level differences using the stationary low-cost Purple Air sensors. Here, the aggregate differences are much stronger. The air quality level is highly statistically different across HOLC risk grades. This probably has to do with the fact, that the Purple Air sensors have a higher spatial resolution as compared to the gridded product. When using the measurements from

[1] $Pollution_n = \boldsymbol{\beta}\, Grade_n + \epsilon_n$ where $Grade_n$ is a set of dummy variables indicating the HOLC grade of neighborhood n.

Figure (4) OLS regression of air pollution on HOLC-grade indicators, with city-FE, clustering on state-level

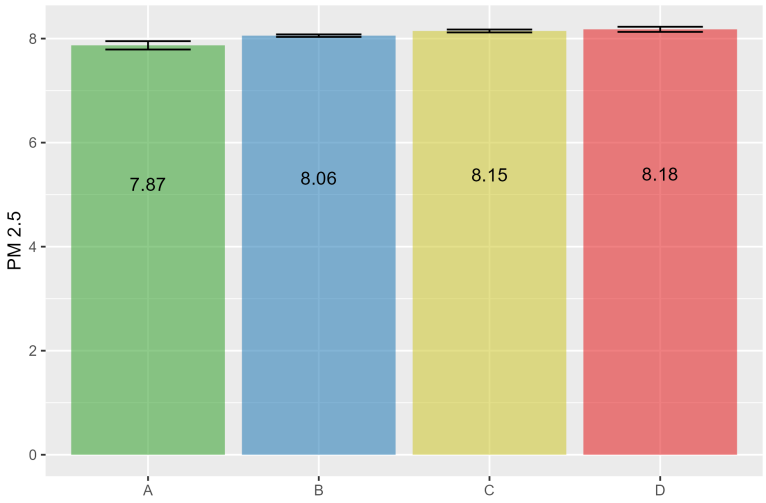

(a) $PM2.5$ from Meng et al. (2019) for 2016

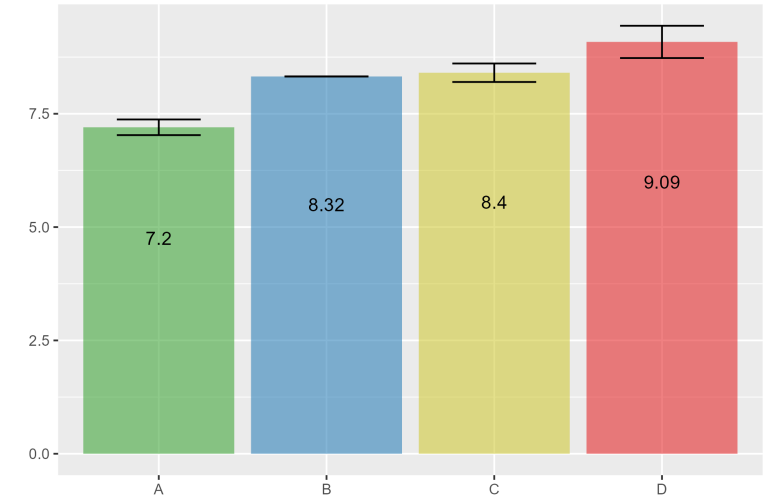

(b) $PM2.5$ from Purple Air Sensors (May 2021 - May 2022)

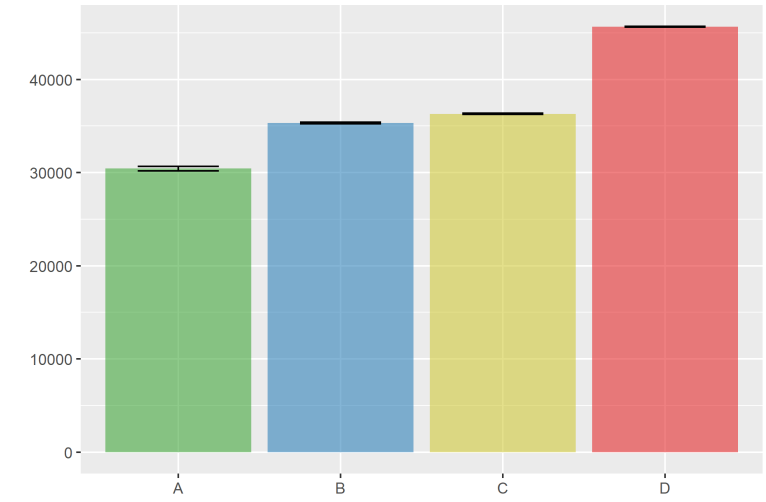

(c) Particle counts per litre from Street View Air Quality

Figure (5) OLS regression of air pollution on HOLC-grade indicators, using pre-cleaned data by Apte et al. (2017), including residential and major arterial traffic

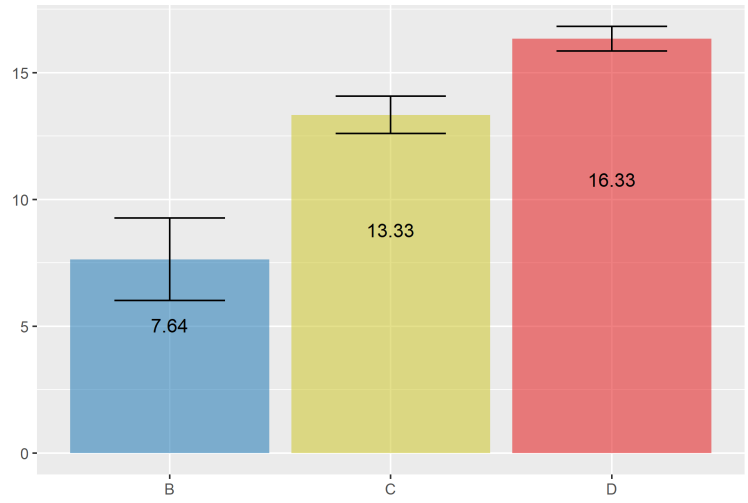

(a) *NO* from Street View Air Quality

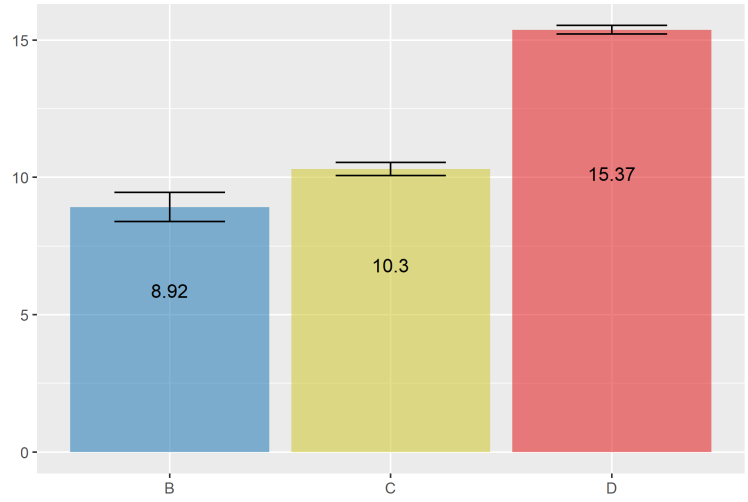

(b) NO_2 from Street View Air Quality

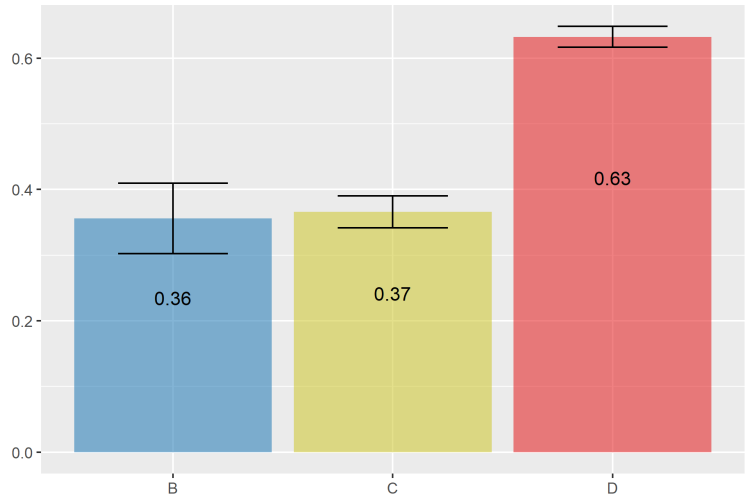

(c) Black Carbon from Street View Air Quality

mobile air quality monitors as displayed in Panel (c), the relative positioning according to HOLC grade of the neighborhood is even clearer: A-graded neighborhoods have the lowest level of PM2.5. Pollution in B- and C-graded neighborhoods range at elevated levels. D-graded neighborhoods see another strong hike in PM2.5.

This pattern is very pronounced also for the other pollutants measured by the mobile sensors, shown in Figure 5. We see a clear ordering for NO, for NO_2 and for Black Carbon. The mobile sensors passed only through B-, C- and D-graded neighborhoods, which is why A-graded neighbordhoods are omitted here.

Table (1) Main results using gridded air pollution product

	Unweighted			Weighted		
	(1)	(2)	(3)	(4)	(5)	(6)
	A-B	B-C	C-D	A-B	B-C	C-D
Comparison	0.01	-0.01	-0.01	0.07	0.00	-0.00
	(0.02)	(0.01)	(0.01)	(0.06)	(0.02)	(0.01)
Treated	0.08*	0.08***	0.02	0.01	0.07**	0.02
	(0.04)	(0.02)	(0.02)	(0.05)	(0.03)	(0.02)
Adjusted R-squared	0.99	0.99	0.99	0.99	0.99	0.99
N	1,558	4,770	6,378	1,558	4,770	6,378

Notes: The treatment estimates are derived from a 400m buffer zone around the respective set of boundaries (A-B, B-C, C-D). The comparison boundaries are based on a 400m buffer zone around grids over each city and weighted by propensity scores to mirror pre-map population characteristics.

Next, we turn toward our main results. The first three columns in Table 1 show the naive unweighted estimates for one point in time 1991. Columns (4) to (6) are the estimates that account for pre-treatment disparities through propensity score weighting. At the comparison boundaries, we do not see any pollution disparities. At the eventually treated boundaries, however, we estimate that the lower-graded side has a higher pollution level as compared to the higher-graded side. For instance, at B-C boundaries, the C-buffer has 0.08 higher level of PM2.5 in the unweighted estimates (column 2). Even when weighting according to propensity score, the pollution level remains at similar magnitude and statistically significant at 10-percent level (column 5). The statistical significance vanished for A-B boundaries. At C-D boundaries we do not detect any statistically significant pollution difference. The effect size correponds to about 1/50 of a standard deviation, which probably has to do with the coarseness of the gridded pollution data.

How did the disparity evolve over time? Figure 6 shows estimates from separate regressions at B-C boundaries for 5-year intervals. The data reach as far back as 1981. For that year, the treated boundaries have a much larger pollution disparity, although, the effect is not statistically significant owing to noise in the data as reflected by the large confidence intervals. From 1986, the pollution disparities at the treated boundaries are statistically significant from the comparison boundaries. The effect size gets smaller, most likely thanks to the Clean Air Act, but the disparity remains even until today.

Figure (6) Results on B-C boundaries over time

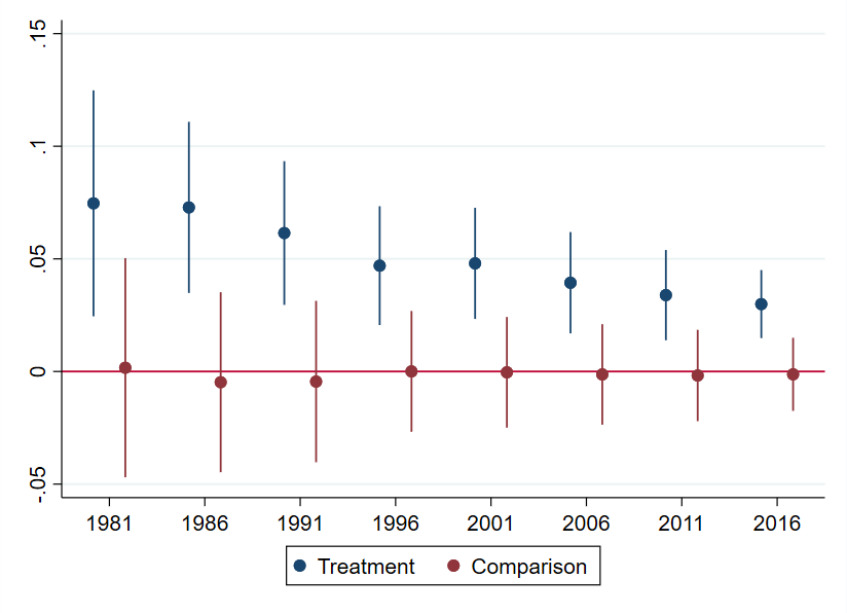

Notes: The treatment estimates are derived from a 400m buffer zone around the respective set of boundaries (A-B, B-C, C-D). The comparison boundaries are based on a 400m buffer zone around grids over each city and weighted by propensity scores to mirror pre-map population characteristics. Here, separately for 5-year intervals.

Table (2) Results from mobile measurements: Ultra Fine Particles

	Unweighted			Weighted		
	(1)	(2)	(3)	(4)	(5)	(6)
	A-B	B-C	C-D	A-B	B-C	C-D
lgs=1	-3417	-1358	-389	-3430	-1218	1468
	(2538)	(634)	(1134)	(2105)	(308)	(1426)
treat=1 × lgs=1		7322*	7943*		7181**	6086
		(634)	(1134)		(308)	(1426)
Adjusted R-squared	0.50	0.62	0.64	0.51	0.59	0.63
N	74	182	288	74	182	288

Notes: Mean value is 37 000 (particle count). Effect corresponds to 1/10 of the mean.

We now turn towards the preliminary results using the mobile air pollution measurements. PM2.5 is expressed as counts per 1 liter of air. Table 2 shows estimates for Ultra Fine Particles smaller than 0.1 mikrometer in size. The mobile measurements are only available in three Californian cities San Francisco, Oakland and Los Angeles. Again, B-C boundaries have elevated particle counts on the lower-graded side of treated boundaries. This corresponds to roughly one tenth of the mean of UFP count.

We conduct various robustness checks, but the picture remains consistent across many specifications: i) Using 1930 and 1940 characteristics separately or jointly to detect the treatment propensities ii) Keeping also non-straight boundary segments, iii) using actual HOLC same-grade boundaries as comparison boundaries.

5 Conclusion

We set out to examine the consequences of a discriminatory housing policy in the US of the 1930s on long-lasting ethnic pollution disparities. The correlative results across whole neighborhoods and the preliminary naive results around HOLC boundaries are suggestive of enduring pollution disparities.

In the next step, we request data access to the 1940 full-count census, and apply the described methodology using propensity methods to test whether the policy had a causal effect. We, furthermore, aim to provide evidence on the mechanisms connecting the historical policy to modern day outcomes. The prime candidates are the siting of polluting industrial plants (Currie et al., 2015) and the construction and expansion of the federal highway system that started in the 1950s (Nall and O'Keeffe, 2018; Brinkman and Lin, 2020).

References

Alexeeff, S. E., Roy, A., Shan, J., Liu, X., Messier, K., Apte, J. S., Portier, C., Sidney, S. and Van Den Eeden, S. K. (2018), 'High-resolution mapping of traffic related air pollution with Google street view cars and incidence of cardiovascular events within neighborhoods in Oakland, CA', *Environmental Health: A Global Access Science Source* **17**(1), 1–13.

Apte, J. S., Messier, K. P., Gani, S., Brauer, M., Kirchstetter, T. W., Lunden, M. M., Marshall, J. D., Portier, C. J., Vermeulen, R. C. and Hamburg, S. P. (2017), 'High-Resolution Air Pollution Mapping with Google Street View Cars: Exploiting Big Data', *Environmental Science and Technology* **51**(12), 6999–7008.

Ash, M. and Boyce, J. K. (2018), 'Racial disparities in pollution exposure and employment at US industrial facilities', *Proceedings of the National Academy of Sciences of the United States of America* **115**(42), 10636–10641.

Barkjohn, K., Gantt, B., VonWald, I. and Clements, A. (2019), PurpleAir PM2.5 performance across the U.S., Technical report, EPA.

Bassi, V., Kahn, M. E., Lozano Gracia, N., Porzio, T. and Sorin, J. (2021), 'Pollution in Ugandan Cities: Do Managers Avoid it or Adapt in Place?', *SSRN Electronic Journal* .

Baum-Snow, N. (2020), 'Urban transport expansions and changes in the spatial structure of u.S. cities: Implications for productivity and welfare', *Review of Economics and Statistics* **102**(5), 929–945.

Brinkman, J. and Lin, J. (2020), 'Freeway Revolts! The Quality of Life Effects of Highways', (March).

California EPA (2021), 'Pollution and Prejudice: Redlining and Environmental Injustice in California'.
URL: *https://storymaps.arcgis.com/stories/f167b251809c43778a2f9f040f43d2f5*

Colmer, J., Hardman, I., Shimshack, J. and Voorheis, J. (2020), 'Disparities in PM2.5 air pollution in the United States', *Science* **369**(6503), 575–578.

Currie, J., Davis, L., Greenstone, M. and Reed, W. (2015), 'Environmental health risks and housing values: Evidence from 1,600 toxic plant openings and closings', *American Economic Review* **105**(2), 678–709.

Feenstra, B., Collier-Oxandale, A., Papapostolou, V., Cocker, D. and Polidori, A. (2020), 'The AirSensor open-source R-package and DataViewer web application for interpreting community data collected by low-cost sensor networks', *Environmental Modelling and Software* **134**(August), 104832.
URL: *https://doi.org/10.1016/j.envsoft.2020.104832*

Fishback, P., Rose, J., Snowden, K. and Storrs, T. (2021), 'New Evidence on Redlining by Federal Housing Programs in the 1930s', *NBER Working Paper* pp. 2013–2015.

Gillingham, K. and Huang, P. (2021), 'Racial Disparities in the Health Effects From Air Pollution: Evidence From Ports', *SSRN Electronic Journal* .

Hoffman, J. S., Shandas, V. and Pendleton, N. (2020), 'The effects of historical housing policies on resident exposure to intra-urban heat: A study of 108 US urban areas', *Climate* **8**(1), 1–15.

Liu, J., Clark, L. P., Bechle, M. J., Hajat, A., Kim, S. Y., Robinson, A. L., Sheppard, L., Szpiro, A. A. and Marshall, J. D. (2021), 'Disparities in Air Pollution Exposure in the United States by Race/Ethnicity and Income, 1990-2010', *Environmental health perspectives* **129**(12), 127005.

Meng, J., Li, C., Martin, R. V., Van Donkelaar, A., Hystad, P. and Brauer, M. (2019), 'Estimated Long-Term (1981-2016) Concentrations of Ambient Fine Particulate Matter across North America from Chemical Transport Modeling, Satellite Remote Sensing, and Ground-Based Measurements', *Environmental Science and Technology* **53**(9), 5071–5079.

Nall, C. and O'Keeffe, Z. P. (2018), 'What Did Interstate Highways Do to Urban Neighborhoods ?', *Working Paper* .

Namin, S., Xu, W., Zhou, Y. and Beyer, K. (2020), 'The legacy of the Home Owners' Loan Corporation and the political ecology of urban trees and air pollution in the United States', *Social Science and Medicine* **246**(November 2019).

Nardone, A., Casey, J. A., Morello-Frosch, R., Mujahid, M., Balmes, J. R. and Thakur, N. (2020), 'Associations between historical residential redlining and current age-adjusted rates of emergency department visits due to asthma across eight cities in California: an ecological study', *The Lancet Planetary Health* **4**(1), e24–e31.

Nardone, A., Casey, J. A., Rudolph, K. E., Karasek, D., Mujahid, M. and Morello-Frosch, R. (2020), 'Associations between historical redlining and birth outcomes from 2006 through 2015 in California', *PLoS ONE* **15**(8 August), 1–18.
URL: *http://dx.doi.org/10.1371/journal.pone.0237241*

Riddell, C. A., Goin, D. E., Morello-Frosch, R., Apte, J. S., Glymour, M. M., Torres, J. M. and Casey, J. A. (2022), 'Hyper-localized measures of air pollution and risk of preterm birth in Oakland and San Jose, California', *International Journal of Epidemiology* **50**(6), 1875–1885.

Rothstein, R. (2017), *The Color of Law A Forgotten History of How Our Government Segregated America*, Liveright.

Tessum, C. W., Apte, J. S., Goodkind, A. L., Muller, N. Z., Mullins, K. A., Paolella, D. A., Polasky, S., Springer, N. P., Thakrar, S. K., Marshall, J. D. and Hill, J. D. (2019), 'Inequity in consumption of goods and services adds to racial-ethnic disparities in air pollution exposure', *Proceedings of the National Academy of Sciences of the United States of America* **116**(13), 6001–6006.

Tryner, J., L'Orange, C., Mehaffy, J., Miller-Lionberg, D., Hofstetter, J. C., Wilson, A. and Volckens, J. (2020), 'Laboratory evaluation of low-cost PurpleAir PM monitors and in-field correction using co-located portable filter samplers', *Atmospheric Environment* **220**, 117067.
URL: *https://doi.org/10.1016/j.atmosenv.2019.117067*

A Appendix

Figure (7) Boyle Heights area in LA

Notes: Case study of Boyle Heights area in LA

Figure (8) East LA Interchange

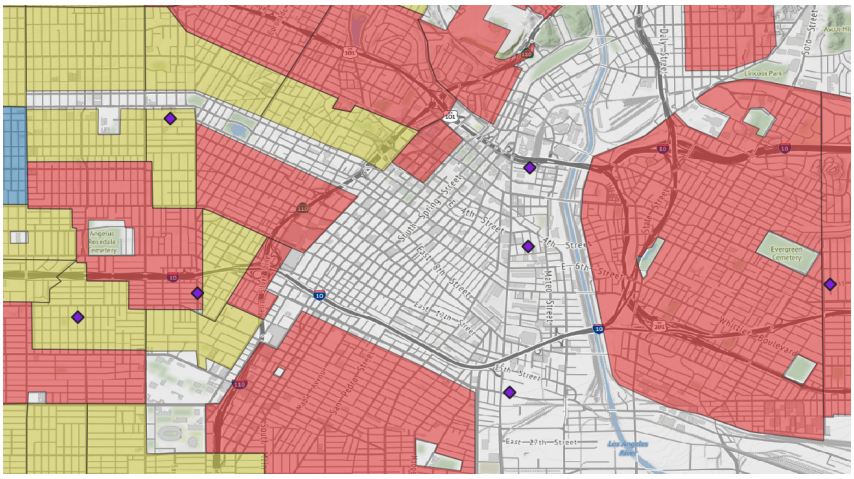

Notes: L.A. City Map (2020) with HOLC polygons (1939)

Figure (9) HOLC map 1939 LA

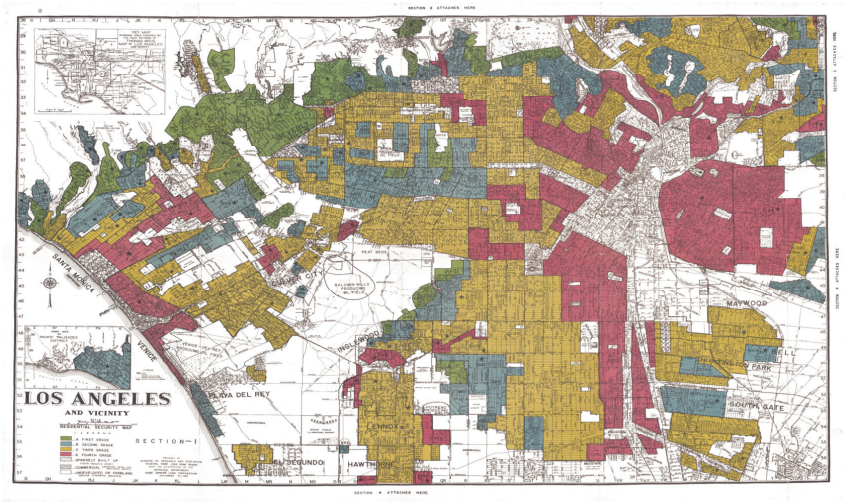

Notes:

Table (3) Treatment likelihood

	(1) A-B	(2) B-C	(3) C-D
treat			
Gap in immigrant share	15.81***	7.42***	4.36**
	(5.35)	(1.66)	(1.95)
Gap in black share	10.45**	4.20***	1.84**
	(4.19)	(1.44)	(0.76)
Gap in Socio-economic indicator	-0.00	-0.02***	-0.05***
	(0.01)	(0.00)	(0.01)
Pseudo R-squared			
N	389	1,140	1,193

Notes: Probit estimation of treatment status. Variables reflect gaps in population characteristics in 1940 along both treatment and comparison boundaries. City-FE included. Standard errors account for correlation at the city-level. *** p<0.01, ** p<0.05, * p<0.1

Figure (10) HOLC area description 1939 LA

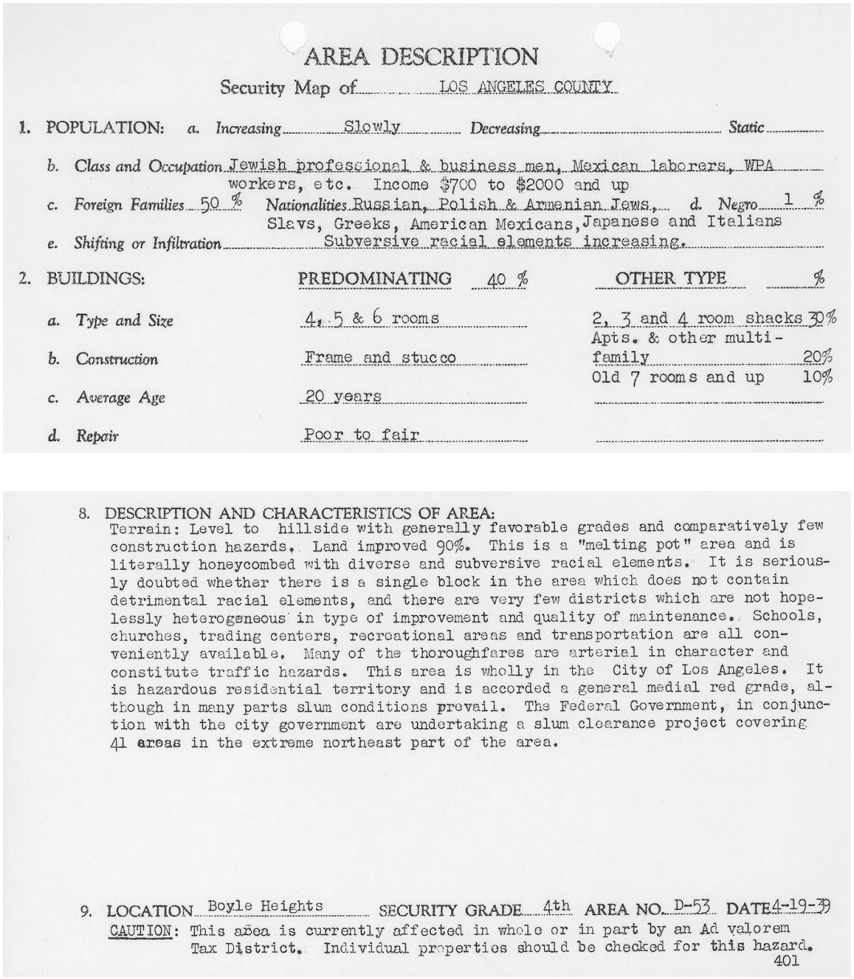

AREA DESCRIPTION

Security Map of LOS ANGELES COUNTY

1. POPULATION: a. *Increasing* Slowly *Decreasing* *Static*

b. *Class and Occupation* Jewish professional & business men, Mexican laborers, WPA workers, etc. Income $700 to $2000 and up

c. *Foreign Families* 50 % *Nationalities* Russian, Polish & Armenian Jews, d. *Negro* 1 % Slavs, Greeks, American Mexicans, Japanese and Italians

e. *Shifting or Infiltration* Subversive racial elements increasing.

2. BUILDINGS:	PREDOMINATING 40 %	OTHER TYPE %
a. *Type and Size*	4, 5 & 6 rooms	2, 3 and 4 room shacks 30%
b. *Construction*	Frame and stucco	Apts. & other multi-family 20%
c. *Average Age*	20 years	Old 7 rooms and up 10%
d. *Repair*	Poor to fair	

8. DESCRIPTION AND CHARACTERISTICS OF AREA:
Terrain: Level to hillside with generally favorable grades and comparatively few construction hazards. Land improved 90%. This is a "melting pot" area and is literally honeycombed with diverse and subversive racial elements. It is seriously doubted whether there is a single block in the area which does not contain detrimental racial elements, and there are very few districts which are not hopelessly heterogeneous in type of improvement and quality of maintenance. Schools, churches, trading centers, recreational areas and transportation are all conveniently available. Many of the thoroughfares are arterial in character and constitute traffic hazards. This area is wholly in the City of Los Angeles. It is hazardous residential territory and is accorded a general medial red grade, although in many parts slum conditions prevail. The Federal Government, in conjunction with the city government are undertaking a slum clearance project covering 41 areas in the extreme northeast part of the area.

9. LOCATION Boyle Heights SECURITY GRADE 4th AREA NO. D-53 DATE 4-19-39

CAUTION: This area is currently affected in whole or in part by an Ad valorem Tax District. Individual properties should be checked for this hazard.

401

Figure (11) Grid approach: illustration

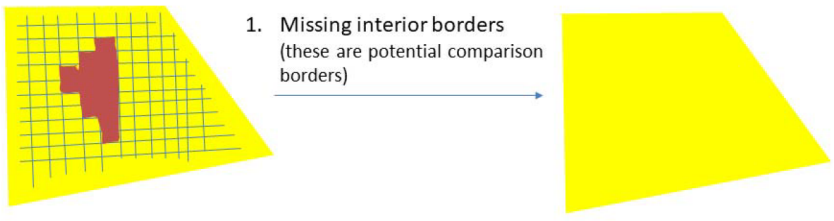

Notes: From **?**

Figure (12) Idiosyncratic border approach: illustration

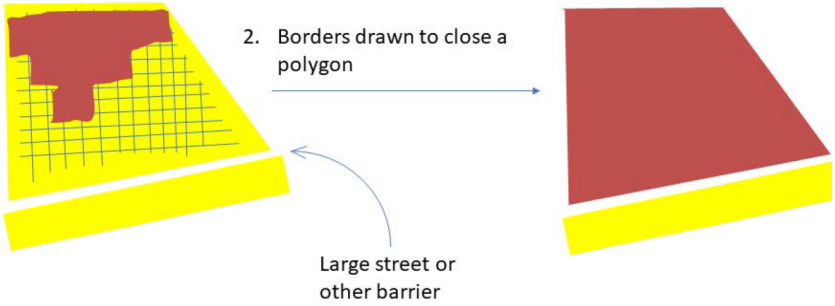

Notes: From **?**

Figure (13) Hyper-local measuring of air quality

(a) Purple Air Sensor

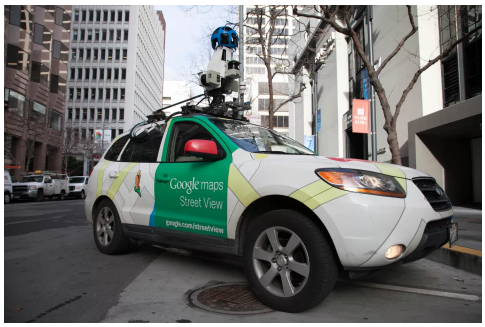

(b) Street View Air Quality

Figure (14) HOLC Purple Air Sensors

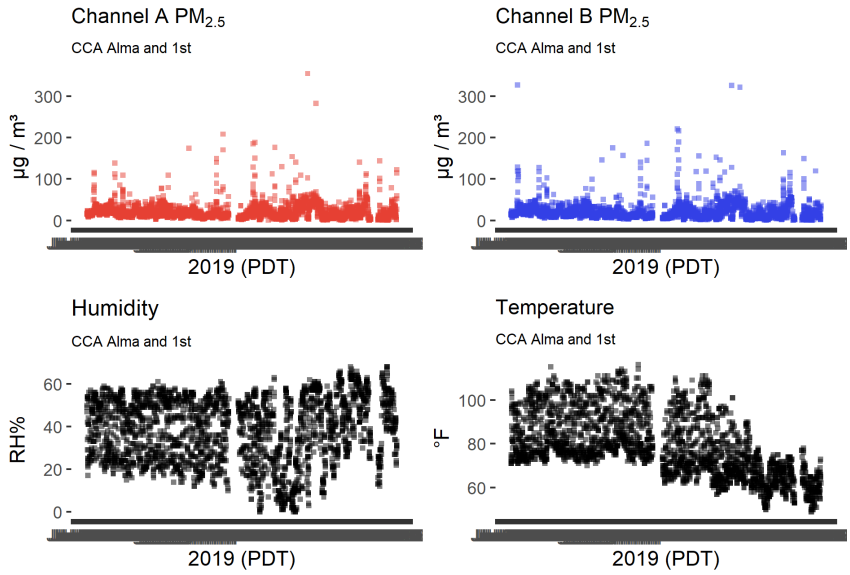

Notes: Example for measurements by one stationary Purple Air sensor, located in Los Angeles.

Figure (15) Street View Air Quality: Time Series

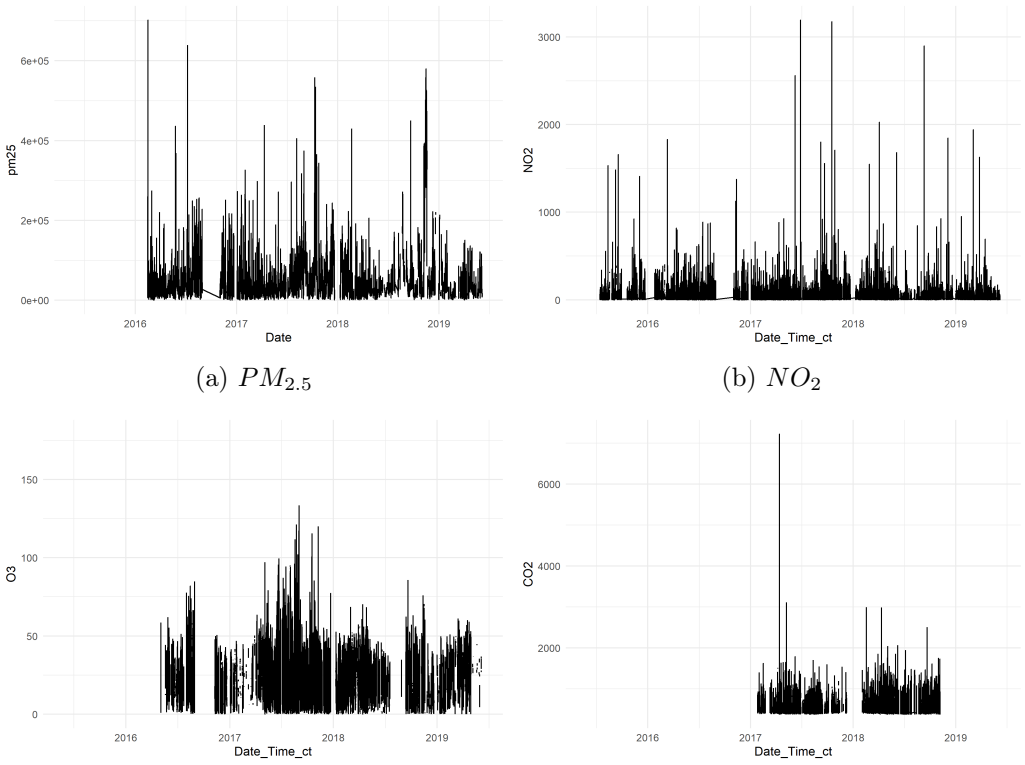

(a) $PM_{2.5}$ (b) NO_2

(c) O_3 (d) CO_2

Notes: Time series of pollutants as measured by the mobile sensors.

Figure (16) Coverage

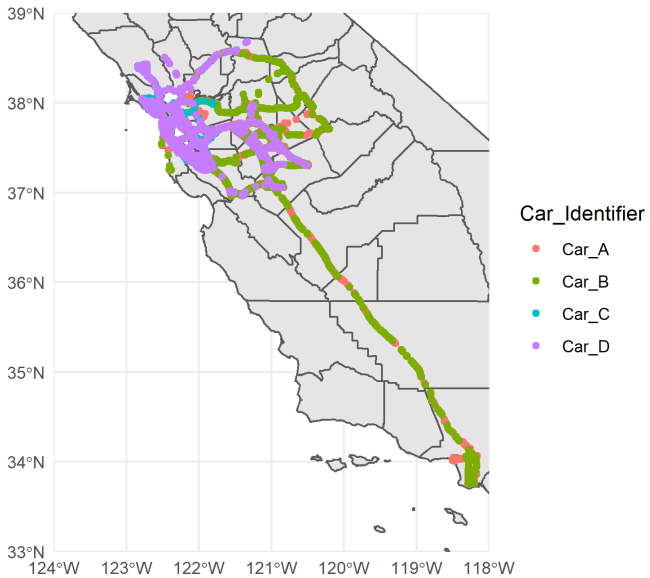

Notes: Regional coverage of mobile sensor measurements for the four measurement vehicles.

Figure (17) Street View Air Quality: San Francisco Coverage

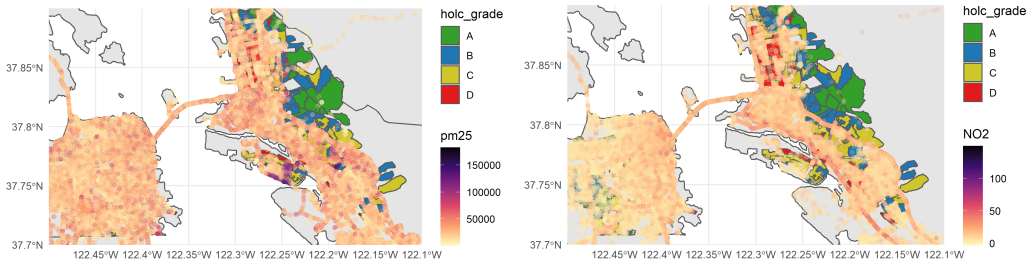

(a) PM2.5 (b) NO2

Notes: The map shows the measurements in the San Francisco/Bay Area for PM2.5 (left, counts per liter volume) and for NO2 (right, parts per billion).

Figure (18) NO_2 from Street View Air Quality and Speed

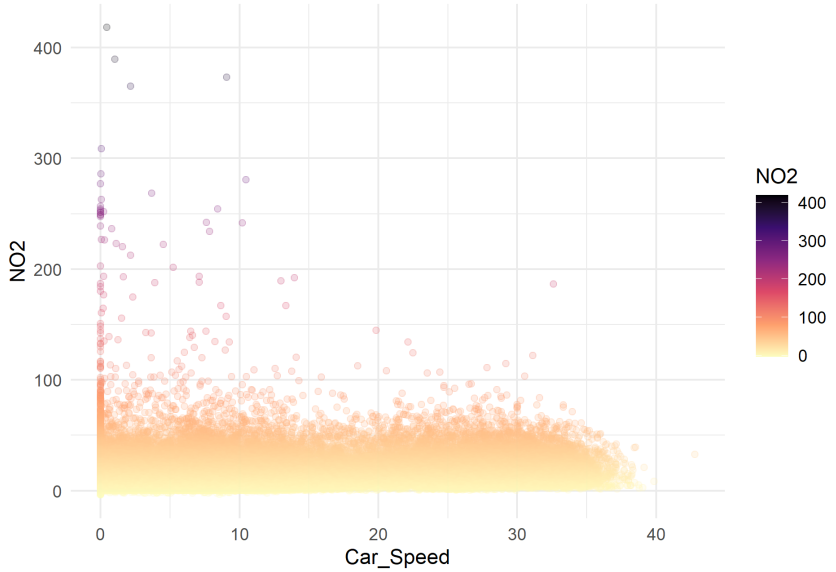

Notes: The graph plots the relationship between speed and NO2 measurements for one vehicle.

Figure (19) Purple Air vs. Street View

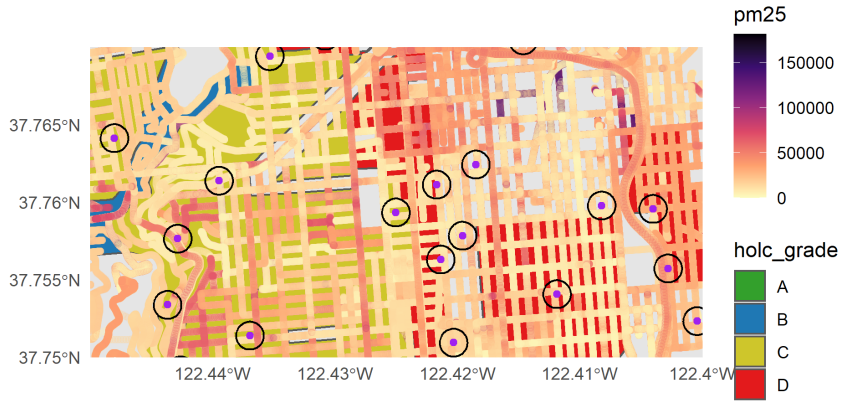

Notes: Purple points with 100m buffer indicate the location of Purple Air sensors, yellow-orange-purple color scale on roads indicate the pollution contamination measured by Google Street View vehicles.

Figure (20) Mean outcomes for segregation and housing

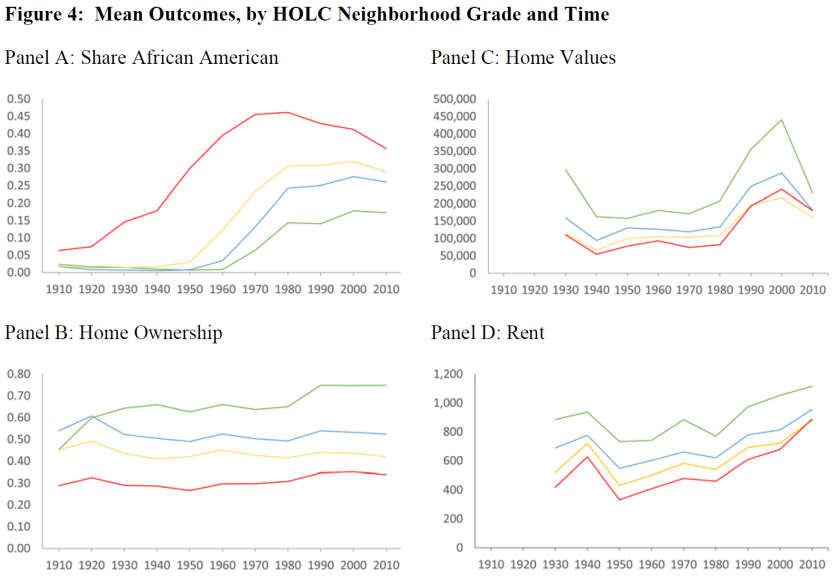

*Notes:*From **?**

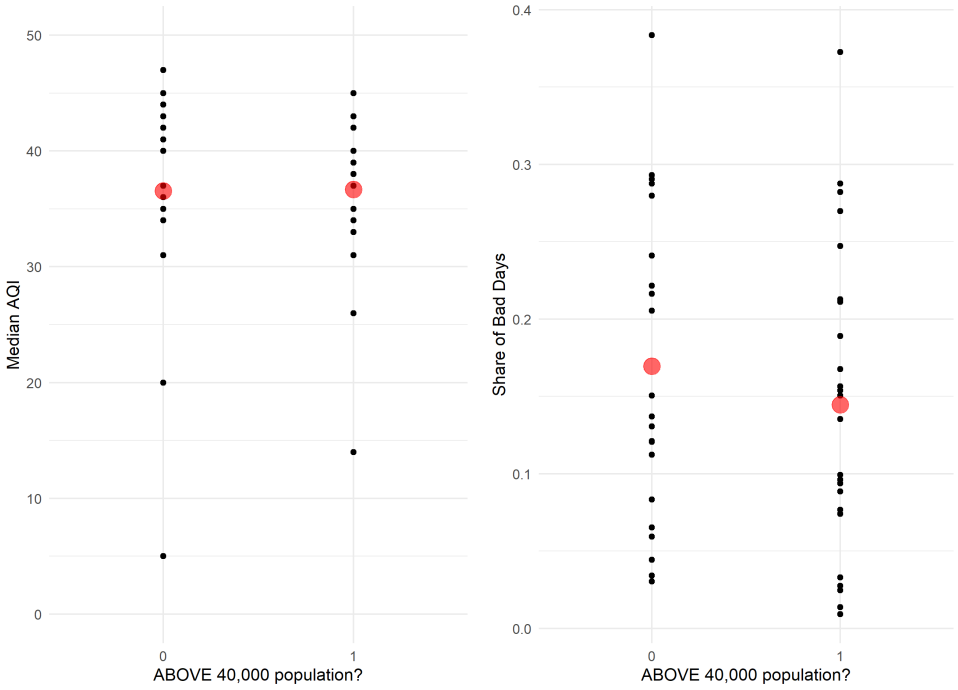

(a) (b)

A.1 Pop. cut-off

Empirical Strategy: City-level 40,000 Population Cutoff

Exploit program discontinuity: HOLC maps were only drawn for cities with population $>$ 40,000.

Compare cities above the cut-off with cities below the cutoff

Main assumption requires continuity of variables around the population size cut-off

$$Treat = \begin{cases} \textbf{1} \text{ if } 50,000 > pop_{1930} \geq 40,000 \\ \textbf{0} \text{ if } 30,000 \leq pop_{1930} < 40,000 \end{cases}$$

Limitations: i. low power, ii. external validity

Results of 40,000 population cut-off